Rescue of neuronal migration deficits in a mouse model of fetal Minamata disease by increasing neuronal Ca^{2+} spike frequency

Jennifer K. Fahrion[a,1], Yutaro Komuro[a,1], Ying Li[a], Nobuhiko Ohno[a], Yoav Littner[a], Emilie Raoult[b,c], Ludovic Galas[c], David Vaudry[b,c], and Hitoshi Komuro[a,2]

[a]Department of Neurosciences, Lerner Research Institute, Cleveland Clinic Foundation, Cleveland, OH 44195; [b]Institut National de la Santé et de la Recherche Médicale Unit 982, Différenciation et Communication Neuronale et Neuroendocrine, University of Rouen, Mont-Saint-Aignan, 76821 France; and [c]Cell Imaging Platform of Normandy, Institut National de la Santé et de la Recherche Médicale, Institute for Research and Innovation in Biomedicine, University of Rouen, Mont-Saint-Aignan, 76821 France

Edited by Pasko Rakic, Yale University, New Haven, CT, and approved February 17, 2012 (received for review December 15, 2011)

In the brains of patients with fetal Minamata disease (FMD), which is caused by exposure to methylmercury (MeHg) during development, many neurons are hypoplastic, ectopic, and disoriented, indicating disrupted migration, maturation, and growth. MeHg affects a myriad of signaling molecules, but little is known about which signals are primary targets for MeHg-induced deficits in neuronal development. In this study, using a mouse model of FMD, we examined how MeHg affects the migration of cerebellar granule cells during early postnatal development. The cerebellum is one of the most susceptible brain regions to MeHg exposure, and profound loss of cerebellar granule cells is detected in the brains of patients with FMD. We show that MeHg inhibits granule cell migration by reducing the frequency of somal Ca^{2+} spikes through alterations in Ca^{2+}, cAMP, and insulin-like growth factor 1 (IGF1) signaling. First, MeHg slows the speed of granule cell migration in a dose-dependent manner, independent of the mode of migration. Second, MeHg reduces the frequency of spontaneous Ca^{2+} spikes in granule cell somata in a dose-dependent manner. Third, a unique in vivo live-imaging system for cell migration reveals that reducing the inhibitory effects of MeHg on somal Ca^{2+} spike frequency by stimulating internal Ca^{2+} release and Ca^{2+} influxes, inhibiting cAMP activity, or activating IGF1 receptors ameliorates the inhibitory effects of MeHg on granule cell migration. These results suggest that alteration of Ca^{2+} spike frequency and Ca^{2+}, cAMP, and IGF1 signaling could be potential therapeutic targets for infants with MeHg intoxication.

abnormal neuronal migration | congenital methylmercury poisoning

During periods of fetal and early postnatal development, exposure to methylmercury (MeHg) induces congenital intoxication, leading to the development of characteristic neurological symptoms, including mental retardation, cerebellar ataxia, and cerebral palsy (1–3). This medical phenomenon is known as fetal Minamata disease (FMD). Characteristic neuropathological changes in patients with FMD include (*i*) bilateral cerebral atrophy and hypoplasia with a decrease in the number of cortical neurons; (*ii*) underdevelopment of neurons, including small somata and short dendrites; (*iii*) cerebellar atrophy and hypoplasia with a reduction of the cerebellar granule cell layer; (*iv*) hypoplasia of the corpus callosum; (*v*) dysmyelination of white matter; and (*vi*) hydrocephalus (4–8). These abnormalities suggest that MeHg causes multiple deficits in neurons and glia, including abnormal migration, differentiation, and growth (9, 10). There is no effective therapy available for FMD patients.

MeHg exposure remains a major public health concern because of the natural and anthropogenic release of inorganic mercury into the aquatic environment, where it is biotransformed by algae and bacteria into MeHg (11, 12). MeHg can pass along the food chain, leading to humans through consumption of MeHg-contaminated fish. Once inside the body of pregnant women, MeHg readily crosses the placental and blood–brain barriers with a direct toxic effect on the fetus (13, 14). The fetus is known to serve as a "mercury trap" in pregnant women. The concentration of mercury in the fetal brain is at least twice that of the mother's (5). In addition to placental transfer, developing infants can also be exposed to mercury via breastfeeding (15).

The most susceptible brain region to MeHg-mediated injury is the cerebellum, with high susceptibility in cerebellar granule cells and the cerebrum (3, 16, 17). Previous studies demonstrate that there are large numbers of ectopic cerebellar granule cells in the brains of FMD patients (1–8), suggesting that cerebellar granule cells are highly vulnerable to MeHg exposure. The most vulnerable period of cerebellar development in humans for MeHg exposure is during the third trimester (18). The equivalent time of development in mice is during the first two postnatal weeks (19). In this study, using a mouse model of FMD, we examined how MeHg affects the migration of cerebellar granule cells during early postnatal development. MeHg exposure induces changes in the activity of a wide range of signaling molecules (20–23), including elevations of oxidative stress, which often leads to apoptotic cell death (24, 25). The question of which signaling molecules play crucial roles in the effects of MeHg on neuronal cell migration remains to be determined. Using in vitro and in vivo assays for monitoring cell movement, we revealed that MeHg inhibits the migration of granule cells in a dose-dependent manner, independent of the mode of migration. The inhibitory effects of MeHg on granule cell migration are ameliorated by increasing somal Ca^{2+} spike frequencies via controlling Ca^{2+}, cAMP, and IGF1 signaling.

Results

MeHg Inhibits Granule Cell Translocation in the Developing Cerebellum. After final cell division, granule cells migrate from their origin, the top of the external granular layer (EGL), to their final destination within the internal granular layer (IGL) (Fig. 1*A*) (26–28). The use of BrdU, which is incorporated only into proliferating cells (such as granule cell precursors), demonstrates the chronology of granule cell translocation in early postnatal mouse cerebella. Postnatal 8-d-old (P8) mice were i.p. injected with 50 μg/g body weight (bw) BrdU. Two hours after injection, the BrdU-labeled cells were localized at the top of the EGL, where granule cell precursors proliferate (Fig. 1*B*). One day after injection (P9), the BrdU-labeled cells were detected throughout

Author contributions: J.K.F. and H.K. designed research; J.K.F., Y.K., Y. Li, and H.K. performed research; J.K.F., Y.K., N.O., Y. Littner, E.R., L.G., D.V., and H.K. analyzed data; and J.K.F. and H.K. wrote the paper.

The authors declare no conflict of interest.

This article is a PNAS Direct Submission.

[1]J.K.F. and Y.K. contributed equally to this work.

[2]To whom correspondence should be addressed. E-mail: komuroh@ccf.org.

This article contains supporting information online at www.pnas.org/lookup/suppl/doi:10.1073/pnas.1120747109/-/DCSupplemental.

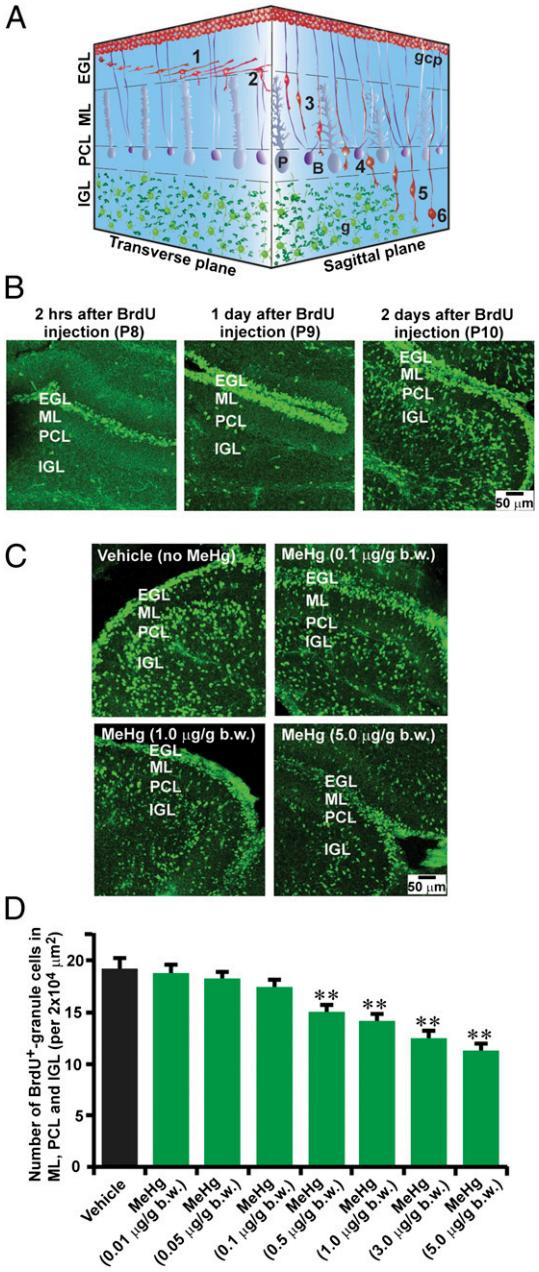

Fig. 1. MeHg inhibits granule cell translocation in the early postnatal mouse cerebellum. (*A*) 3D representation of granule cell migration in the developing cerebellum. (1) Tangential migration in the EGL; (2) turning near the EGL-ML border; (3) Bergmann glia-associated radial migration in the ML; (4) stationary state in the PCL; (5) glia-independent radial migration in the IGL; (6) completion of migration in the IGL. B, Bergmann glia; g, post-migratory granule cell; gcp, granule cell precursor; P, Purkinje cell. (*B*) Time course of granule cell translocation in vivo. At 2 h (P8), 1 d (P9), and 2 d (P10) after injection of BrdU (50 μg/g bw), the distribution of BrdU-labeled cells was analyzed in sagittal sections of cerebella. (*C*) The effects of MeHg on the translocation of BrdU-labeled cells in the cerebella. Mouse pups were i.p. injected with three different doses (0.1, 1.0, 5.0 μg/g bw) of MeHg over 4 d (P6–P9). The control group of mice was injected with only vehicle. At P8, the pups were i.p. injected with BrdU (50 μg/g bw). At P10, the distribution of BrdU-labeled cells in sagittal sections of cerebella was examined. (*D*) Histogram showing the reduction in the number of BrdU-labeled cells in the ML, PCL, and IGL by MeHg (0.01, 0.05, 0.1, 0.5, 1.0, 3.0, or 5.0 μg/g bw) for 4 d (P6–P9). Each column represents the average value obtained from at least 10,000 cells. Bars represent SD. $^{**}P < 0.01$ indicates statistical significance.

the EGL (Fig. 1*B*). Two days after injection (P10), >50% of BrdU-labeled cells left the EGL and translocated their soma into the molecular layer (ML), Purkinje cell layer (PCL), and IGL (Fig. 1*B*).

First, we examined whether MeHg affects this translocation of granule cells. Mouse pups were i.p. injected with seven different doses (0.01, 0.05, 0.1, 0.5, 1.0, 3.0, and 5.0 μg/g bw) of MeHg for four consecutive days (P6–P9). The exposure to these levels of MeHg did not induce noticeable changes in the activity of spontaneous movement and did not cause death of the animals. All pups were i.p. injected with a single dose of BrdU (50 μg/g bw) during the exposure period, on P8. The analysis of the distribution of BrdU-labeled cells revealed that MeHg exposure over P6–P9 reduces the number of BrdU-labeled cells in the ML, PCL, and IGL of P10 cerebella in a dose-dependent manner (Fig. 1 *C* and *D*). The average number of BrdU-labeled cells in the ML, PCL, and IGL was reduced by 22% with 0.5 μg/g bw MeHg, by 27% with 1.0 μg/g bw MeHg, by 35% with 3.0 μg/g bw MeHg, and by 42% with 5.0 μg/g bw MeHg (Fig. 1*D*).

The reduction of the number of BrdU-labeled cells in the ML, PCL, and IGL may be due to increased cell death of granule cells and granule cell precursors caused by MeHg. A TUNEL assay indicated that low to moderate levels (0.01–1.0 μg/g bw) of MeHg do not alter the number of $TUNEL^+$ cells in the EGL, whereas higher levels (3.0–5.0 μg/g bw) of MeHg increase the number (Fig. S1).

These results suggest that the reduction of the number of BrdU-labeled cells in the ML, PCL, and IGL by moderate levels (0.5–1.0 μg/g bw) of MeHg is due to the inhibition of granule cell translocation, whereas the reduction of the number by high levels (3.0–5.0 μg/g bw) of MeHg is due to the inhibition of translocation as well as the increase in cell death.

MeHg Slows Granule Cell Migration Independent of the Mode of Migration. The inhibition of granule cell translocation by MeHg suggests that it may inhibit granule cell migration. To test this possibility, we used real-time observation of cell movement and found that the addition of 10 μM MeHg immediately slowed the speed of radial migration of a granule cell from 28.3 μm/h to 6.0 μm/h in the ML of a cerebellar slice obtained from P10 mice (Fig. 2 *A* and *B*). These results indicate that MeHg decelerates the speed of granule cell migration. During the migration toward their final destination, granule cells exhibit three different modes of migration: (*i*) tangential migration in the EGL; (*ii*) Bergmann glia-associated radial migration in the ML; and (*iii*) glia-independent radial migration in the IGL. The inhibitory effects of MeHg on granule cell migration may depend on the mode of migration. To test this possibility, we determined the effects of MeHg on granule cell migration in the EGL, ML, and IGL. MeHg inhibited granule cell migration in all three cortical layers in a dose-dependent manner (Fig. S2). For example, 20 μM MeHg reduced the speed of granule cell migration in the EGL by 62%, in the ML by 57%, and in the IGL by 52% (Fig. 2*C*), suggesting that MeHg inhibits the migration of granule cells independent of the mode of migration.

MeHg Reduces the Motility of Granule Cells. The deceleration of granule cell migration by MeHg may result from a decrease in granule cell motility or in alterations to the surrounding environment, such as cell–cell interactions. To determine this issue, we examined the effects of MeHg on the migration of isolated granule cells. Time-lapse recordings of cell movement in microexplant cultures of P0–P3 mouse cerebella demonstrated that 10 μM MeHg slows the migration of isolated granule cells (from 56.4 μm/h to 31.6 μm/h in cell-α, and from 45.3 μm/h to 18.6 μm/h in cell-β) (Fig. 2 *D* and *E*). The addition of MeHg at concentrations ranging from 1.0 to 20.0 μM slowed the movement of isolated granule cells in a dose-dependent manner (Fig. S3). The average speed of migration was reduced by 16% with 1.0 μM MeHg, 21% with 5.0 μM MeHg, 27% with 10.0 μM MeHg, and 33% with 20.0 μM MeHg (Fig. 2*F*). These results suggest that MeHg

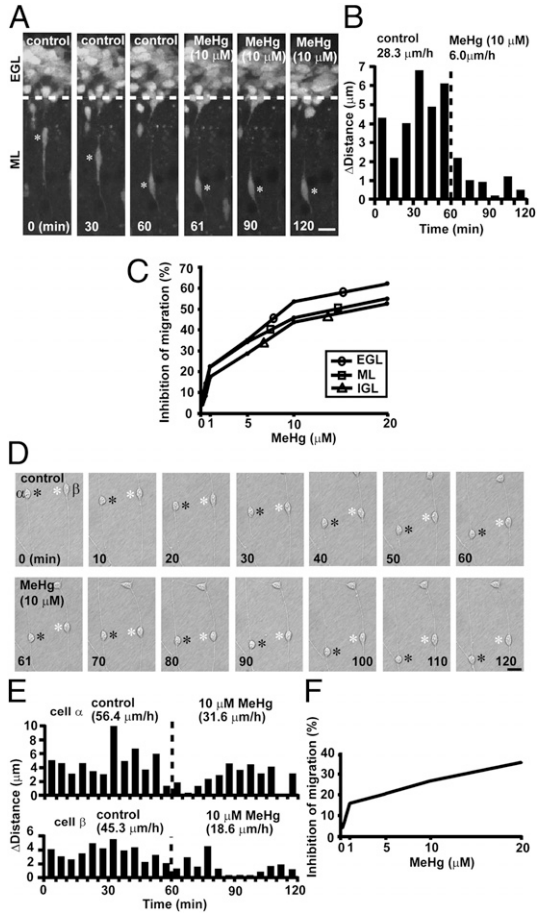

Fig. 2. MeHg slows granule cell migration in vitro. (*A*) Time-lapse images showing that 10 μM MeHg inhibits the radial migration of a granule cell in the ML of a cerebellar slice obtained from a P10 mouse. Asterisks mark the granule cell soma. Elapsed time is indicated on the bottom of each photograph. (Scale bar: 12 μm.) (*B*) Sequential changes in the distance traveled during each 10-min interval by the granule cell shown in *A* were plotted as a function of elapsed time before and after the application of 10 μM MeHg. (*C*) Inhibition of the speed of granule cell migration in the EGL, ML, and IGL by MeHg (0.1–20.0 μM). (*D*) Time-lapse images showing that 10 μM MeHg slows the migration of isolated granule cells in the microexplant cultures of P3 mouse cerebella. Black and white asterisks mark the somata of migrating granule cells. Elapsed time is indicated on the bottom of each photograph. (Scale bar: 12 μm.) (*E*) Sequential changes in the distance traveled by two granule cells (α and β shown in *D*) during each 5-min interval were plotted as a function of elapsed time before and after the application of 10 μM MeHg. (*F*) Inhibition of the speed of migration in the microexplant cultures by MeHg (0.1–20.0 μM).

directly reduces the motility of granule cells. A comparison of data obtained from the experiments using cerebellar slices and microexplant cultures indicates that MeHg causes stronger inhibitory effects on granule cell migration in the cerebellar slices than those in the microexplant cultures. The differences suggest that alterations to the surrounding environment may also play a role in MeHg-induced deceleration of granule cell migration.

MeHg Reduces Ca^{2+} Spike Frequency of Granule Cells. Our working hypothesis was that MeHg slows granule cell migration by altering Ca^{2+} signaling, because it has been shown that MeHg disrupts intracellular Ca^{2+} homeostasis and reduces N-type Ca^{2+} channel currents in granule cells (20, 29). It has been reported that granule cell migration is highly sensitive to changes in Ca^{2+} signaling pathways (30, 31) and that the inhibition of N-type Ca^{2+} channels slows migration (32). Time-lapse imaging of intracellular Ca^{2+} levels revealed that 10 μM MeHg reduces the frequency of spontaneous Ca^{2+} spikes in a granule cell soma (Fig. 3*A*). The effects of MeHg on Ca^{2+} spike frequency in granule cell somata were dose dependent (Fig. 3*B*). The average frequency of Ca^{2+} spikes was reduced by 12% with 0.5 μM MeHg, 19% with 1.0 μM MeHg, 26% with 5.0 μM MeHg, 33% with 10.0 μM MeHg, and 41% with 20.0 μM MeHg. These results suggest that MeHg may slow the migration of granule cells by reducing Ca^{2+} spike frequency, because it has been shown that changes in Ca^{2+} spike frequency correspond linearly with changes in the speed of granule cell migration (30, 31).

Reducing the Effect of MeHg on Ca^{2+} Spike Frequency Reduces the Inhibitory Effects of MeHg on Granule Cell Migration. If MeHg inhibits granule cell migration by reducing Ca^{2+} spike frequency, experimental enhancement of Ca^{2+} spike frequency may therefore reduce the inhibitory effect of MeHg on granule cell migration. To test this possibility, we focused on the role of Ca^{2+}, cAMP, and IGF1 signaling because it has been reported that these signaling pathways are involved in the control of Ca^{2+} spike frequency (30, 31, 33) and are affected by MeHg exposure (20, 34, 35). We used 10 μM MeHg, because the application of this amount of MeHg induces a significant deceleration of the speed of granule cell migration (Fig. 2 *C* and *F*), although prolonged application

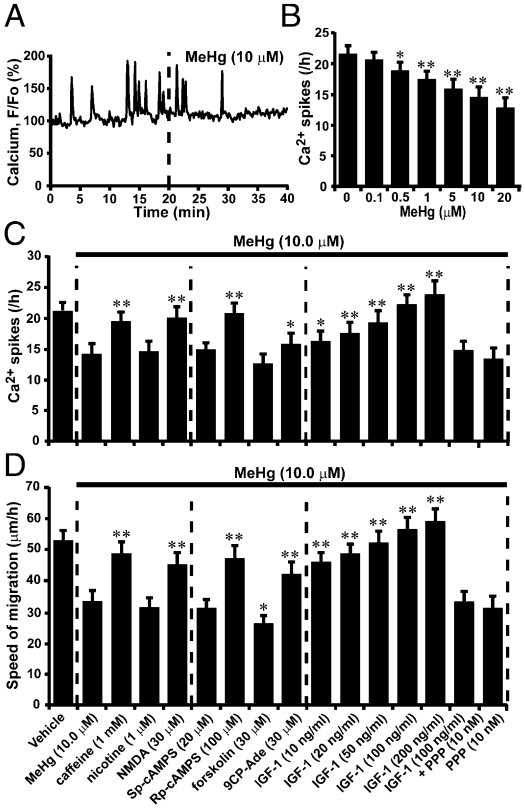

Fig. 3. Reduction of the effects of MeHg on the speed of granule cell migration by increasing Ca^{2+} spike frequency through controlling Ca^{2+}, cAMP, and IGF1 signaling pathways. (*A*) Reduction of the recurrence of spontaneous Ca^{2+} spikes in granule cell soma by 10 μM MeHg. (*B*) Histograms showing a dose-dependent reduction in the frequency of Ca^{2+} spikes in granule cell somata by MeHg. Each column represents the average frequency of Ca^{2+} spikes obtained from at least 50 migrating cells. Bars represent SD. (*C and D*) Changes in the effects of MeHg (10 μM) on (*C*) Ca^{2+} spike frequency of granule cells and (*D*) the speed of migration by caffeine, nicotine, NMDA, Sp-cAMPS, Rp-cAMPS, forskolin, 9CP-Ade, IGF1, IGF1 + PPP, or PPP. In *C* and *D*, each column represents the average values obtained from at least 50 migrating cells. Bars represent SD. $*P < 0.05$ and $**P < 0.01$ indicate statistical significance.

affects the viability of granule cells (36). In the case of Ca^{2+} signaling, caffeine (stimulator of internal Ca^{2+} release through ryanodine receptors, 1 mM) or NMDA (agonist of the NMDA-type glutamate receptors, 30 μM) markedly reduced the effect of MeHg on Ca^{2+} spike frequency of granule cells (Fig. 3*C*). In contrast, nicotine (agonist of nicotinic acetylcholine receptors, 1 μM) did not alter the effect of MeHg on Ca^{2+} spike frequency (Fig. 3*C*). In the case of cAMP signaling, Rp-cAMPS (a competitive cAMP antagonist, 100 μM) reduced the inhibitory effects of MeHg on Ca^{2+} spike frequency, whereas Sp-cAMPS (a competitive cAMP agonist, 20 μM) did not significantly alter the effect (Fig. 3*C*). Likewise, 9CP-Ade (adenylyl cyclase inhibitor, 30 μM) reduced the effect of MeHg on Ca^{2+} spike frequency, whereas forskolin (adenylyl cyclase stimulator, 30 μM) did not significantly alter the effect (Fig. 3*C*). In the case of IGF1 signaling, IGF1 at concentrations between 10–200 ng/mL eliminated the effect of MeHg on Ca^{2+} spike frequency in a dose-dependent manner (Fig. 3*C*). Picropodophyllin (PPP, a specific IGF1 receptor inhibitor, 10 nM) alone did not alter the effects of MeHg on Ca^{2+} spike frequency, but it completely blocked the effect of IGF1 on MeHg-induced reduction of Ca^{2+} spike frequency (Fig. 3*C*).

Next, we determined whether the reduced inhibitory effect of MeHg on Ca^{2+} spike frequency produced by manipulating Ca^{2+}, cAMP, and IGF1 signaling results in the reduction in the inhibitory effect of MeHg on granule cell migration. First, caffeine and NMDA markedly reduced the inhibitory effects of MeHg on the speed of migration (Fig. 3*D*). In contrast, nicotine had little effect on the effects of MeHg on migration (Fig. 3*D*). Second, Rp-cAMPS reduced the inhibitory effect of MeHg on the speed of migration, whereas Sp-cAMPS did not significantly alter the effect (Fig. 3*D*). Similarly, 9CP-Ade reduced the effect of MeHg on the speed of migration, and forskolin enhanced the effect (Fig. 3*D*). Third, IGF1 completely reversed the inhibitory effect of MeHg on the speed of migration (Fig. 3*D*). The effects of IGF1 on MeHg-induced deceleration of migration were eliminated by PPP, but PPP alone did not significantly alter the effects of MeHg on migration (Fig. 3*D*). These results indicate that reducing the inhibitory effect of MeHg on Ca^{2+} spike frequency reduces the inhibitory effect of MeHg on granule cell migration, suggesting that alterations in Ca^{2+} spike frequency play crucial roles in the effects of MeHg on granule cell migration.

Inhibition of Granule Cell Translocation by MeHg Is Ameliorated by Manipulating Ca^{2+}, cAMP, and IGF1 Signaling. The present in vitro studies have indicated that manipulating Ca^{2+}, cAMP, and cGMP signaling pathways might reduce the inhibitory effects of MeHg on granule cell translocation in the developing cerebellum. To test this possibility, we i.p. injected four different doses (0.5, 1.0, 3.0, and 5.0 μg/g bw) of MeHg into mouse pups for two consecutive days (P8–P9). Immediately after injection of MeHg, the pups were also injected with caffeine (2 μg/g bw), Rp-cAMPS (0.4 μg/g bw), 9CP-Ade (0.4 μg/g bw), or IGF1 (5 μL, 100 ng/mL) into the subarachnoid space between the skull and the surface of the cerebellum for two consecutive days (P8–P9). At P8, we i.p. injected BrdU (50 μg/g bw) into all pups. Analysis of the distribution of BrdU-labeled cells revealed that at all levels of MeHg exposure, caffeine, Rp-cAMPS, or IGF1 reduced the inhibitory effect of MeHg on the number of BrdU-labeled cells in the ML, PCL, and IGL of P10 mouse cerebella, whereas 9CP-Ade did not significantly alter the effects (Fig. 4 *A–D*). These results suggest that manipulating Ca^{2+}, cAMP, and IGF-1 signaling pathways mitigates the inhibitory effects of MeHg on granule cell translocation in early postnatal mouse cerebella.

Manipulating Ca^{2+}, cAMP, and IGF1 Signaling Reduces the Effects of MeHg on the Speed of Granule Cell Migration in Vivo. The next question we addressed was whether manipulating Ca^{2+}, cAMP, and cGMP signaling changes the effects of MeHg on the speed of granule cell migration in the developing cerebellum. Using a newly developed in vivo live-imaging system for cell migration, we monitored the effect of MeHg on the speed of granule cell

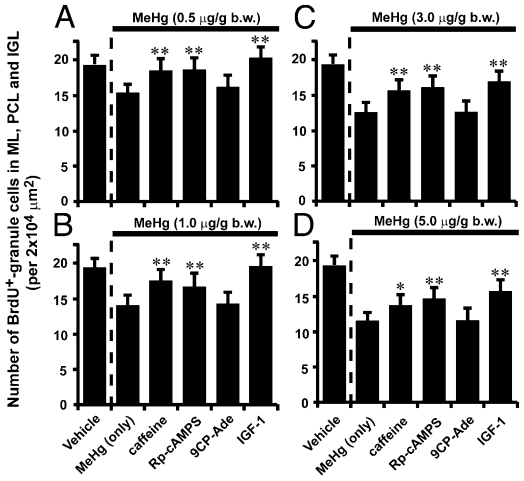

Fig. 4. Reduction of the inhibitory effects of MeHg on granule cell translocation in P10 mouse cerebella by caffeine, Rp-cAMPS, 9CP-Ade, and IGF1. (*A–D*) Histograms showing the reduction of the effects of MeHg (0.5 μg/g bw in *A*, 1.0 μg/g bw in *B*, 3.0 μg/g bw in *C*, and 5.0 μg/g bw in *D*) on the number of BrdU-labeled cells in the ML, PCL, and IGL by caffeine (2 μg/g bw), Rp-cAMPS (0.4 μg/g bw), 9CP-Ade (0.4 μg/g bw), or IGF1(5 μL, 100 ng/mL). Each column represents the average value obtained from at least 10,000 cells. Bars represent SD.

migration in the mouse cerebellum in a real-time manner. A small amount of 1,1′-dioctadecyl-3,3,3′,3′ tetramethylindocarbocyanine perchlorate (DiI) solution was injected into the EGL of lobules V, VI, and VII of P10 mouse cerebella (Fig. 5*A*). Two hours after injection, we observed the migration of DiI-labeled granule cells in the EGL using confocal microscopy (Fig. 5 *B* and *C*). Time-lapse recordings of cell movement revealed that the injection of MeHg (10 μL, 20 μM) into the dorsal surface of the cerebellum slowed the tangential migration of DiI-labeled granule cell in the EGL (Fig. 5 *D–F*). Importantly, when caffeine (2 μg/g bw) and MeHg (10 μL, 20 μM) were simultaneously injected into the dorsal surface of the cerebellum, the inhibitory effects of MeHg on the speed of granule cell migration in the EGL were markedly ameliorated (Fig. 5 *G–J*). Likewise, the injection of Rp-cAMPS (0.4 μg/g bw), 9CP-Ade (0.4 μg/g bw), or IGF1 (5 μL, 100 ng/mL) into the dorsal surface of the cerebellum noticeably reduced the inhibitory effect of MeHg (10 μL, 20 μM) on the speed of granule cell migration in the EGL (Fig. 5*J*). These results suggest that MeHg-induced deceleration of granule cell migration in the developing cerebellum can be ameliorated by manipulating Ca^{2+}, cAMP, and IGF1 signaling.

Discussion

In this study, we examined the effects of MeHg on the migration of cerebellar granule cells, because pathological examination of the brains of FMD patients suggests that MeHg impairs neuronal cell migration (9, 10). The present study indicates that MeHg inhibits granule cell migration by reducing the frequency of somal Ca^{2+} spikes through alterations in Ca^{2+}, cAMP, and IGF1 signaling.

In this study, exposure to >0.5 μg/g bw MeHg at P6–P9 resulted in inhibition of granule cell translocation in P10 mouse cerebella. It has been reported that the total Hg in the brains of MeHg exposed patients in the Minamata Bay area in Japan was 10–15 μg/g (7), and that the application of 10 μg/g bw per day MeHg during early postnatal periods results in increases in total Hg levels to 20 μg/g in rat brains at P10 (37). The levels of MeHg (0.01–5.0 μg/g bw per day) used in this in vivo study may be considered to be within low to middle levels for MeHg poisoning, but may be higher than those estimated from the ingestion or inhalation of MeHg, which occurs during normal daily life (38). The half-life of excretion of MeHg is ∼70 d in humans and ∼8 d in mice (39). After demethylation of MeHg takes place in the brain, inorganic

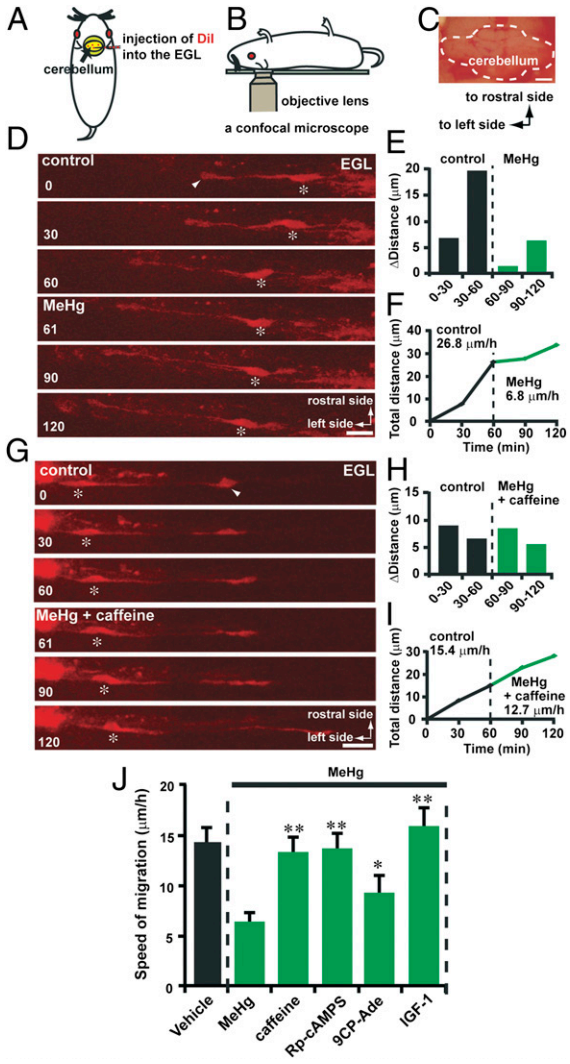

Fig. 5. Reduction of the inhibitory effects of MeHg on the speed of granule cell migration in vivo by caffeine, Rp-cAMPS, 9CP-Ade, and IGF1. (*A* and *B*) Procedure for DiI injection into the EGL of the cerebellum (*A*) and monitoring granule cell migration in vivo using confocal microscopy (*B*). (*C*) Photograph showing the dorsal surface of a P10 mouse cerebellum. (Scale bar: 1,100 μm.) (*D*) Time-lapse images showing that MeHg (10 μL, 20 μM) slowed the tangential migration of a DiI-labeled granule cell in the EGL of the P10 mouse cerebellum. In *D* and *G*, asterisks and arrowheads mark the granule cell somata and the tip of the leading processes. Elapsed time (in min) is indicated on the bottom-left corner of each photograph. (Scale bars: *D*, 15 μm; *G*, 16 μm). (*E* and *F*) Sequential changes in (*E*) the distance traveled during each 30 min interval and (*F*) the total distance traveled by the granule cell shown in *D* were plotted as a function of elapsed time before and after the application of MeHg (10 μL, 20 μM). (*G*) Time-lapse images showing that caffeine (2 μg/g bw) reduces the effects of MeHg (10 μL, 20 μM) on the speed of granule cell migration in the EGL of the P10 mouse cerebellum. (*H* and *I*) Sequential changes in (*H*) the distance traveled during each 30 min interval and (*I*) the total distance traveled by the granule cell shown in *G* were plotted as a function of elapsed time before and after the application of MeHg (10 μL, 20 μM) and caffeine (2 μg/g bw). (*J*) Reduction of the effects of MeHg (10 μL, 20 μM) on the speed of granule cell migration in the EGL of P10 mouse cerebella by caffeine (2 μg/g bw), Rp-cAMPS (0.4 μg/g bw), 9CP-Ade (0.4 μg/g bw), and IGF1 (5 μL, 100 ng/mL). Each column represents the average values obtained from at least 40 migrating cells. Bars represent SD.

mercury has a very long half-life (39). The present results may provide a template for estimating the effects of MeHg on neuronal cell migration in the developing brain. Because the excretion of mercury (specifically, inorganic mercury) is very slow, it is reasonable to speculate that chronic exposure to MeHg during a prolonged period of fetal and postnatal development results in deficits in granule cell migration even at considerably lower doses. The lowest chronic exposure of MeHg needed to produce adverse effects on neuronal cell migration is still unknown.

The present study indicates that Ca^{2+} spike frequency is one of the primary targets of MeHg-induced inhibition of granule cell migration. Ca^{2+} spikes (or transient Ca^{2+} elevations) are known to play an essential role in maintaining the movement of cells ranging from fibroblasts to immature neurons (30, 31, 40). The inhibition of Ca^{2+} spikes by buffering of intracellular Ca^{2+} levels reduces or inhibits cell movement (41). There are several possible explanations for how MeHg causes the inhibition of granule cell migration through reducing Ca^{2+} spike frequency. First, it has been reported that Ca^{2+} spikes play a critical role in organizing the assembly and disassembly of cytoskeletal components, which is essential for cell movement (42). Therefore, changes in Ca^{2+} spike frequency by MeHg may inhibit granule cell migration by disrupting the assembly and disassembly of cytoskeletal components. Second, the inhibition of Ca^{2+} spikes by MeHg may interfere in the formation of focal adhesion by altering the activity of phosphorylated focal adhesion kinase, leading to the impairment of granule cell adhesion to the surrounding tissues. Third, it has been shown that at their final phase of migration, in the absence of external signals, granule cells reduce Ca^{2+} spike frequency and stop the recurrence of Ca^{2+} spikes immediately before termination of movement (31). These results suggest that MeHg may turn on an internal switch, which is responsible for the termination of granule cell migration, by reducing Ca^{2+} spike frequency.

The cellular mechanisms by which MeHg reduces Ca^{2+} spike frequency may be complex. MeHg may simultaneously alter multiple upstream- and downstream-targets of Ca^{2+} signaling, including the activity of voltage-dependent Ca^{2+} channels and internal Ca^{2+} stores (20, 29). Furthermore, MeHg may alter the expression levels of Ca^{2+} channels and Ca^{2+} signaling molecules. It has been shown that MeHg alters the ontogeny of specific isoforms of protein kinase C (downstream target of Ca^{2+} signaling) and its regional activity (43). At present, we cannot rule out the role of other ions and ion channels in the MeHg-induced reduction of Ca^{2+} spike frequencies, because it has been shown that MeHg affects the activity of Na^+, K^+, and Cl^- channels (21, 44, 45), which are able to alter Ca^{2+} signaling. We also cannot exclude the possibility that changes in steady-state Ca^{2+} levels play a role in MeHg-induced inhibition of granule cell migration through altering Ca^{2+} spike frequency.

MeHg exposure affects the growth of the liver (39), which is the primary organ for the production of IGF1 (46). It may be possible that MeHg inhibits granule cell migration by decreasing endogenous IGF1 levels through the inhibition of liver growth. The relationship between MeHg exposure, IGF1 levels in the brain, and IGF1 production in the liver needs to be examined in the future. IGF1 receptors exist at the cell surface as homodimers composed of two identical α/β-monomers or as heterodimers composed of two different receptor monomers (46). To date, little is known about which type of IGF1 receptors are expressed in migrating granule cells.

The present study demonstrates that deficits in granule cell migration produced by short periods of MeHg exposure are rescued by increasing Ca^{2+} spike frequency through the control of Ca^{2+}, cAMP, and IGF1 signaling. Although the question of whether the manipulation of these signaling pathways also ameliorates the adverse effects of chronic MeHg exposure on migration and differentiation of granule cells remains to be answered, the present study sheds light on the role of Ca^{2+} spike frequency and Ca^{2+}, cAMP, and IGF1 signaling in searching for potential therapeutic treatments for infants with MeHg intoxication.

Materials and Methods

Details of materials and methods used are presented in *SI Materials and Methods*.

Animal. Early postnatal CD-1 mice (both sexes) were used in this study. All animal procedures were approved by the Internal Animal Care and Use Committee of the Cleveland Clinic Foundation and the University of Rouen.

Measurement of Granule Cell Translocation Using BrdU. P8 mice were i.p. injected with BrdU (50 μg/g bw). At 2 h, 1 d, and 2 d after BrdU injection, the distribution of BrdU-labeled cells was detected by an anti-BrdU monoclonal antibody (BrdU labeling and Detection Kit I; Boehringer Mannheim).

Observation of Granule Cell Migration in Cerebellar Slices. Cerebella of P10 mice were sectioned into 150-μm-thick slices. To label granule cells, slices were incubated for 4 min in 2 μM CellTracker Green CMFDA (Invitrogen). Using a confocal microscope, images of CellTracker Green CMFDA-labeled granule cells were collected for up to 4 h.

Observation of Granule Cell Migration in Microexplant Cultures. Small pieces of P0–P3 mouse cerebella were placed on 35-mm glass-bottom dishes coated with poly-L-lysine (100 μg/mL)/laminin (20 μg/mL). Each dish was put in a CO_2 incubator. One day after plating, using a confocal microscope, the transmitted images of migrating granule cells at 488 nm were collected.

Ca^{2+} Measurement in Migrating Granule Cells. One day after plating small pieces of P0–P3 mouse cerebella, granule cells were incubated for 30 min with 1 μM Oregon Green 488 BAPTA-1 (Invitrogen). Using a confocal microscope, granule cells loaded with Oregon Green 488 BAPTA-1 were illuminated with a 488-nm light, and fluorescence images at 530 ± 15 nm were collected.

Real-Time Observation of Granule Cell Migration in Vivo. At P10, deep anesthesia was induced by i.p. injection of urethane (1 μg/g bw). A small volume of DiI solution was injected into the EGL of the cerebellum. Two hours after DiI injection, the mice were transferred to the stage of a confocal microscope, and images of DiI-labeled granule cells in the EGL were collected.

Detection of Apoptotic Cell Death. The apoptotic cell death was determined by TUNEL assay kit (Roche Diagnostics).

Statistical Analysis. Statistical comparisons were made using the Student *t* test.

ACKNOWLEDGMENTS. We thank Chris Nelson for critically reading the manuscript. This work was supported by National Institutes of Health Grant R01 ES15612 (to H.K.).

1. Harada M (1964) Neuropsychiatric disturbances due to organic mercury poisoning during the prenatal period. *Psychiat Neuro Japn* 66:426–468.
2. Snyder RD (1971) Congenital mercury poisoning. *N Engl J Med* 284:1014–1016.
3. Eto K (1997) Pathology of Minamata disease. *Toxicol Pathol* 25:614–623.
4. Matsumoto H, Koya G, Takeuchi T (1965) Fetal Minamata disease. A neuropathological study of two cases of intrauterine intoxication by a methyl mercury compound. *J Neuropathol Exp Neurol* 24:563–574.
5. Amin-Zaki L, et al. (1974) Studies of infants postnatally exposed to methylmercury. *J Pediatr* 85:81–84.
6. Eto K, et al. (1992) A fetal type of Minamata disease. An autopsy case report with special reference to the nervous system. *Mol Chem Neuropathol* 16:171–186.
7. Ekino S, Susa M, Ninomiya T, Imamura K, Kitamura T (2007) Minamata disease revisited: An update on the acute and chronic manifestations of methyl mercury poisoning. *J Neurol Sci* 262:131–144.
8. Cace IB, et al. (2011) Relationship between the prenatal exposure to low-level of mercury and the size of a newborn's cerebellum. *Med Hypotheses* 76:514–516.
9. Choi BH, Lapham LW, Amin-Zaki L, Saleem T (1978) Abnormal neuronal migration, deranged cerebral cortical organization, and diffuse white matter astrocytosis of human fetal brain: A major effect of methylmercury poisoning in utero. *J Neuropathol Exp Neurol* 37:719–733.
10. Choi BH (1986) Methylmercury poisoning of the developing nervous system: I. Pattern of neuronal migration in the cerebral cortex. *Neurotoxicology* 7:591–600.
11. Crinnion WJ (2000) Environmental medicine, part three: Long-term effects of chronic low-dose mercury exposure. *Altern Med Rev* 5:209–223.
12. Pirrone N (2001) Mercury research in Europe: Towards the preparation of the EU air quality directive. *Atmos Environ* 35:2979–2986.
13. Lapham LW, et al. (1995) An analysis of autopsy brain tissue from infants prenatally exposed to methylmercury. *Neurotoxicology* 16:689–704.
14. Clarkson TW (1997) The toxicology of mercury. *Crit Rev Clin Lab Sci* 34:369–403.
15. Grandjean P, Jorgensen PJ, Weihe P (1994) Methylmercury from mother's milk: Accumulation in infants. *Environ Health Perspect* 102:74–77.
16. Takeuchi T, et al. (1962) A pathological study of Minamata disease in Japan. *Acta Neuropathol* 2:40–57.
17. Chang LW, Wade PR, Pounds JG, Reuhl KR (1980) Prenatal and neonatal toxicology and pathology of heavy metals. *Adv Pharmacol Chemother* 17:195–231.
18. Marsh DO, et al. (1981) Dose-response relationship for human fetal exposure to methylmercury. *Clin Toxicol* 18:1311–1318.
19. Stringari J, Meotti FC, Souza DO, Santos AR, Farina M (2006) Postnatal methylmercury exposure induces hyperlocomotor activity and cerebellar oxidative stress in mice: Dependence on the neurodevelopmental period. *Neurochem Res* 31:563–569.
20. Sirois JE, Atchison WD (2000) Methylmercury affects multiple subtypes of calcium channels in rat cerebellar granule cells. *Toxicol Appl Pharmacol* 167:1–11.
21. Yuan Y, Atchison WD (2005) Methylmercury induces a spontaneous, transient slow inward chloride current in Purkinje cells of rat cerebellar slices. *J Pharmacol Exp Ther* 313:751–764.
22. Atchison WD, Hare MF (1994) Mechanisms of methylmercury-induced neurotoxicity. *FASEB J* 8:622–629.
23. Farina M, Rocha JB, Aschner M (2011) Mechanisms of methylmercury-induced neurotoxicity: Evidence from experimental studies. *Life Sci* 89:555–563.
24. Polunas M, et al. (2011) Role of oxidative stress and the mitochondrial permeability transition in methylmercury cytotoxicity. *Neurotoxicology* 32:526–534.
25. Farina M, Aschner M, Rocha JB (2011) Oxidative stress in MeHg-induced neurotoxicity. *Toxicol Appl Pharmacol* 256:405–417.
26. Komuro H, Rakic P (1995) Dynamics of granule cell migration: A confocal microscopic study in acute cerebellar slice preparations. *J Neurosci* 15:1110–1120.
27. Komuro H, Rakic P (1998) Distinct modes of neuronal migration in different domains of developing cerebellar cortex. *J Neurosci* 18:1478–1490.
28. Komuro H, Yacubova E, Yacubova E, Rakic P (2001) Mode and tempo of tangential cell migration in the cerebellar external granular layer. *J Neurosci* 21:527–540.
29. Marty MS, Atchison WD (1997) Pathways mediating Ca2+ entry in rat cerebellar granule cells following in vitro exposure to methyl mercury. *Toxicol Appl Pharmacol* 147:319–330.
30. Komuro H, Rakic P (1996) Intracellular Ca^{2+} fluctuations modulate the rate of neuronal migration. *Neuron* 17:275–285.
31. Kumada T, Komuro H (2004) Completion of neuronal migration regulated by loss of $Ca(^{2+})$ transients. *Proc Natl Acad Sci USA* 101:8479–8484.
32. Komuro H, Rakic P (1992) Selective role of N-type calcium channels in neuronal migration. *Science* 257:806–809.
33. Kumada T, Lakshmana MK, Komuro H (2006) Reversal of neuronal migration in a mouse model of fetal alcohol syndrome by controlling second-messenger signalings. *J Neurosci* 26:742–756.
34. Olson FC, Massaro EJ (1980) Developmental pattern of cAMP, adenyl cyclase, and cAMP phosphodiesterase in the palate, lung, and liver of the fetal mouse: Alterations resulting from exposure to methylmercury at levels inhibiting palate closure. *Teratology* 22:155–166.
35. Bulleit RF, Cui H (1998) Methylmercury antagonizes the survival-promoting activity of insulin-like growth factor on developing cerebellar granule neurons. *Toxicol Appl Pharmacol* 153:161–168.
36. Castoldi AF, Barni S, Turin I, Gandini C, Manzo L (2000) Early acute necrosis, delayed apoptosis and cytoskeletal breakdown in cultured cerebellar granule neurons exposed to methylmercury. *J Neurosci Res* 59:775–787.
37. Pan HS, Sakamoto M, Liu XJ, Futatsuka M (2005) Deficits in the brain growth in rats induced by methylmercury treatment during the brain growth spurt. *J Health Sci* 51: 41–47.
38. World Health Organization (1972) Evaluation of methylmercury, lead, cadmium and the food additives amaranth, diethylpyrocarbonate, and octyl gallate, WHO Food Additive Series, No. 4 (WHO, Geneva).
39. Clarkson TW (1972) The pharmacology of mercury compounds. *Annu Rev Pharmacol* 12:375–406.
40. Jaconi ME, et al. (1991) Multiple elevations of cytosolic-free Ca2+ in human neutrophils: Initiation by adherence receptors of the integrin family. *J Cell Biol* 112:1249–1257.
41. Marks PW, Maxfield FR (1990) Transient increases in cytosolic free calcium appear to be required for the migration of adherent human neutrophils. *J Cell Biol* 110:43–52.
42. Feng Y, Walsh CA (2001) Protein-protein interactions, cytoskeletal regulation and neuronal migration. *Nat Rev Neurosci* 2:408–416.
43. Haykal-Coates N, Shafer TJ, Mundy WR, Barone S, Jr. (1998) Effects of gestational methylmercury exposure on immunoreactivity of specific isoforms of PKC and enzyme activity during post-natal development of the rat brain. *Brain Res Dev Brain Res* 109: 33–49.
44. Shafer TJ, Atchison WD (1992) Effects of methylmercury on perineurial Na+ and Ca(2+)-dependent potentials at neuromuscular junctions of the mouse. *Brain Res* 595: 215–219.
45. Yuan Y, et al. (2005) Inwardly rectifying and voltage-gated outward potassium channels exhibit low sensitivity to methylmercury. *Neurotoxicology* 26:439–454.
46. Torres-Aleman I (2010) Toward a comprehensive neurobiology of IGF-I. *Dev Neurobiol* 70:384–396.